

# Nanofriction studies of reactively or non-reactively cluster-eroded single crystal diamond

R. Krämer<sup>a</sup>, Y. Yamaguchi<sup>b</sup>, and J. Gspann<sup>c</sup>

Institut für Mikrostrukturtechnik der Universität Karlsruhe und des Forschungszentrums Karlsruhe, Postfach 3640, 76021 Karlsruhe, Germany

Received 6 September 2004

Published online 13 July 2005 – © EDP Sciences, Società Italiana di Fisica, Springer-Verlag 2005

**Abstract.** Friction properties of cluster-eroded surfaces of synthetic single crystal diamond (Monodite) are compared after erosion with high-speed CO<sub>2</sub> cluster beams as well as with corresponding Ar cluster beams, the cluster impact kinetic energy being 100 keV in both cases. The respective friction values are determined by atomic force microscope measurements. Using CO<sub>2</sub> clusters, the reactive accelerated cluster erosion (RACE) of the single crystal diamond substrates leads to more than seven times higher friction values than those observed after erosion with non-reactive accelerated Ar clusters. Molecular dynamics calculations reveal related differences in the simulations of respective single cluster impacts already at 2 ps after impact.

**PACS.** 36.90.+f Other exotic atoms and molecules; macromolecules; clusters – 62.20.Qp Tribology and hardness – 68.35.Af Atomic scale friction – 81.65.Ps Polishing, grinding, surface finishing – 82.65.+r Surface and interface chemistry; heterogeneous catalysis at surfaces

## 1 Introduction

Friction in the nanometer realm plays a growing role, versus inertia, as the dimensions of mechanical devices shrink to the nanometer scale. As only dry friction is conceivable, diamond with its low friction coefficient is an interesting material. Atomically smooth surfaces may show, in addition, a frictionless, “superlubrous” motion under the intermolecular forces [1,2] which would be of paramount importance for nanomechanical devices.

Cluster erosion has been shown to yield very smooth surfaces [3], with roughness values of the order of 1 nanometer [4,5]. The atomic force microscope is the ideal instrument for studying roughness as well as nanofriction [6].

Here, we compare the nanofriction properties of single crystal diamond cluster-eroded by high-speed impacts of CO<sub>2</sub> clusters, or of Ar clusters, respectively. The two species differ by the presence, or absence, respectively, of a reactive component in the erosion process. While with Ar clusters only physical erosion takes place, with CO<sub>2</sub> clusters the chemical reaction of impact-plasma-activated CO<sub>2</sub> with the carbon substrate leads to an addi-

tional chemical way of erosion. Correspondingly, the process was named RACE (**R**eactive **A**ccelerated **C**luster **E**rosion) [4].

## 2 Experimental

The cluster erosion facility has been described earlier. Clusters are generated by adiabatic expansion of the respective gas through a converging-diverging nozzle of 0.1 mm diameter, 10° angle of initial divergence, and 28 mm length of the diverging part. The source pressures are chosen to yield mean cluster sizes of about 1000 molecules of CO<sub>2</sub>, or atoms of Ar, respectively, according to the known scaling laws. As the molecular weights of 44 for CO<sub>2</sub> and 40 for Ar are comparable, the cluster masses should be comparable, too.

The core of the partly condensed nozzle flow is transferred via two skimming orifices into high vacuum to form the cluster beam. The beam is then partly ionised by impact of 150 eV electrons, focused by up to 10 keV, and accelerated toward the grounded target surface by a 100 keV potential difference. For that purpose, the whole cluster beam source has to be at the corresponding high positive potential. The whole set-up is housed in one common vacuum chamber, whose upper part, at high potential, is electrically separated from the lower part, at ground potential, by an insulating ceramic tube acting as a part of the vacuum chamber wall.

<sup>a</sup> *Present address:* Physik Instrumente (PI), 76228 Karlsruhe/Palmbach, Germany.

<sup>b</sup> *Present address:* Osaka University, Department of Mechanical Engineering, Osaka 565-0871, Japan.

<sup>c</sup> e-mail: juergen.gspann@imt.fzk.de

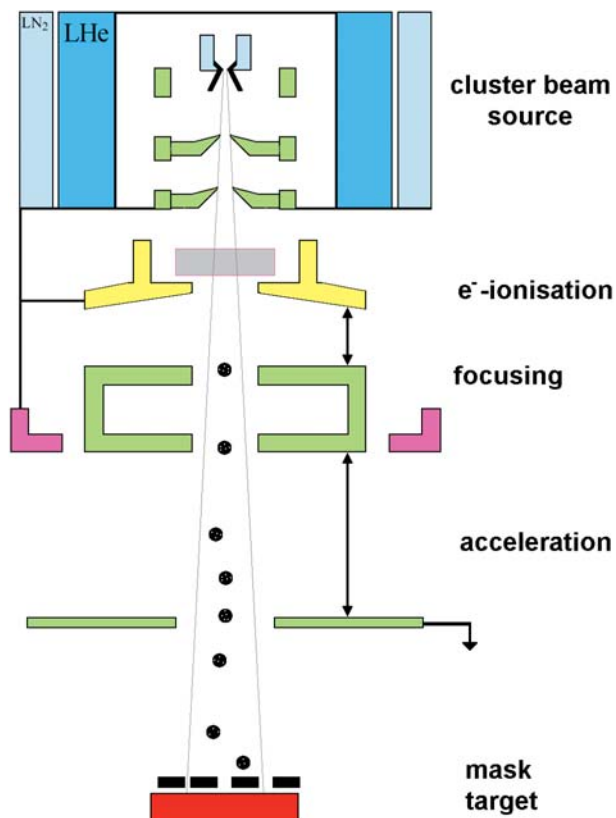


**Fig. 1.** Experimental set-up used for the accelerated cluster erosion with an Ar cluster beam. For use with a CO<sub>2</sub> cluster beam the inner cryostat is filled with liquid nitrogen instead of liquid helium. The whole set-up is housed in a common vacuum chamber.

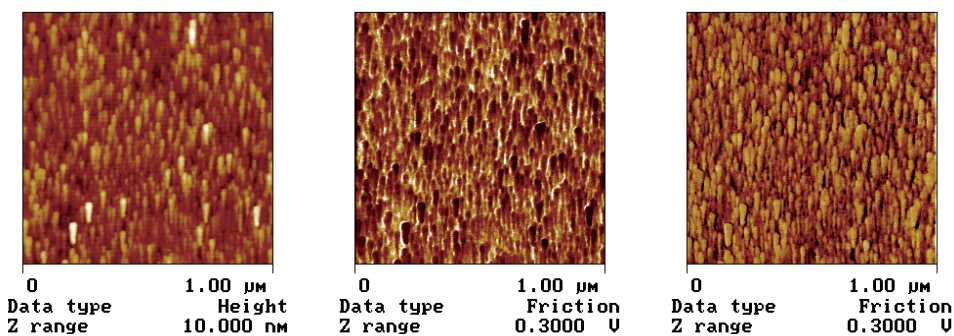


**Fig. 2.** Height image and friction images of the same area of a diamond surface. The friction images are trace ( $x$ -scan) and retrace ( $(-x)$ -scan) images for which the cantilever torsion changes sign. The resulting nearly inverse friction signals still contain a height image contribution.

The outer part of the nozzle flow, containing more than 90% of the nozzle throughput, is pumped by condensation onto bath-cooled cryopanels in the upper high voltage part of the vacuum chamber. Thereby, the instalment of electrical power for pumping is avoided at high electrical potential. While liquid nitrogen cooling is sufficient to condense CO<sub>2</sub>, pumping of Ar requires lower temperatures of the cryopanels. Cooling by liquid helium served for the purpose. Figure 1 shows a schematic view of the cluster erosion facility as used for argon cluster beams. A sequential erosion first by accelerated CO<sub>2</sub> clusters then by accelerated Ar clusters, could be effected without breaking the vacuum.

As erosion masks served 100  $\mu\text{m}$  thick tantal foils with a lapped edge which were placed as tightly as possible onto the diamond specimen. The synthetic single crystal diamond specimen were yellow de Beers Monodite bricks (diamond type Ia) with sawed (100) surfaces.

For investigating the friction of the eroded diamond surfaces an Atomic Force Microscope (AFM) Dimension 3100 (Digital Instruments) was used with a silicon nitride cantilever. The specimen were transferred from the vacuum chamber to the AFM under ambient atmospheric conditions without special precautions. The total erosion time was 50 min, with 30 min CO<sub>2</sub> erosion in the sequential case, in order to establish a stationary situation.

## 3 Results

### 3.1 Friction images of cluster-eroded synthetic diamond

Figure 2 shows height and friction images of cluster-eroded 1  $\mu\text{m} \times 1 \mu\text{m}$  regions. In order to study the nanofriction, the torsion rather than the bending of the AFM cantilever

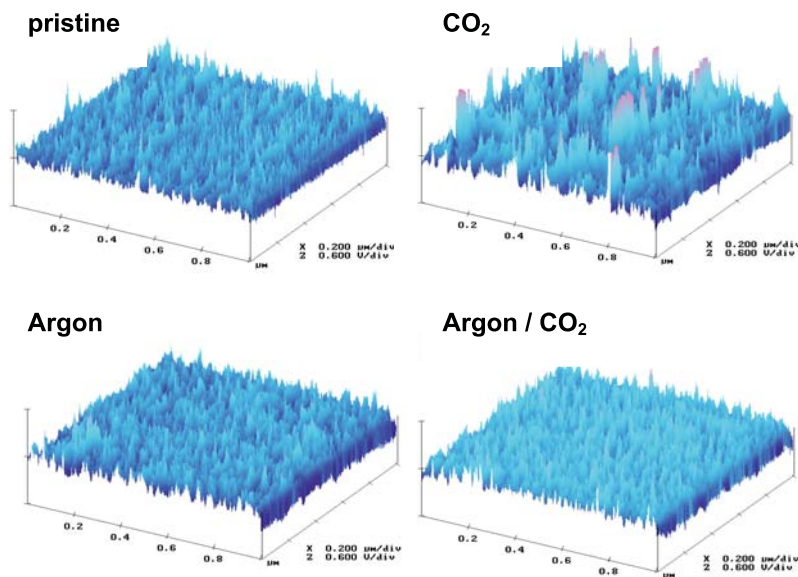


**Fig. 3.** Nanofriction topography of pristine, CO<sub>2</sub> cluster-eroded, Ar cluster-eroded, and sequentially CO<sub>2</sub> and Ar cluster-eroded synthetic diamond. CO<sub>2</sub> cluster erosion leads to the highest friction values.

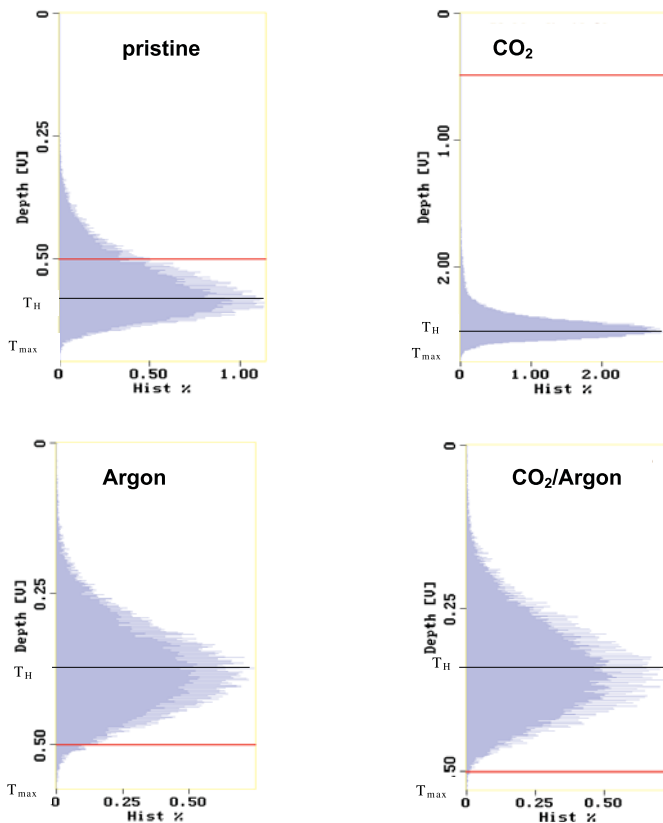


**Fig. 4.** Nanofriction topography evaluation of pristine, CO<sub>2</sub> cluster-eroded, Ar cluster-eroded, and sequentially CO<sub>2</sub> and Ar cluster-eroded synthetic diamond. Heavy lines mark the same value in the various depth scales (0.5 V), while the lighter lines indicate the most probable depths  $T_H$ .

is measured. This torsion reverses sign if the scan direction is reversed.

Therefore, the forward and backward scanning (trace and retrace) yield different friction images which are nearly inverted of each other. However, there is always a

**Table 1.** Nanofriction values, in V, of Ar cluster-eroded, CO<sub>2</sub> cluster-eroded, sequentially CO<sub>2</sub> and Ar cluster-eroded, and pristine (UB) surface areas of a synthetic diamond (100) surface.  $T_{max}$ : maximum depth value of the respective nanofriction topography,  $T_H$ : corresponding most probable value.

	$T_{max}$	$T_H$
Ar	0.57	0.38
CO <sub>2</sub>	2.77	2.5
CO <sub>2</sub> /Ar	<b>0.53</b>	<b>0.35</b>
UB	0.7	0.57

contribution of the bending of the cantilever, which does not reverse sign, since the plane of the detecting laser beam and the axis of the detecting diode field are never perfectly adjusted onto each other. The bending signal being independent of the scan direction, subtracting the retrace friction image from the trace friction image will eliminate the false bending contribution while the friction values are doubled [6].

The corresponding difference friction images provide a nanofriction topography of the respective specimen in contact with the silicon nitride cantilever tip. Figure 3 shows the topographies for the various cluster erosion results.

### 3.2 Friction analysis

The nanofriction topography given by the AFM difference friction data can be statistically evaluated. Peaks in these images indicate high friction.

In Figure 4, histograms of the friction values are given as depth distributions of the respective nanofriction topography. Friction peaks are the higher, the lower the maximum depths are. As the scaling in these diagrams differs considerably, the red lines are given to indicate a common value, 0.5 V. Table 1 shows a summary of the maximum and the most probable depth values for the various surfaces.

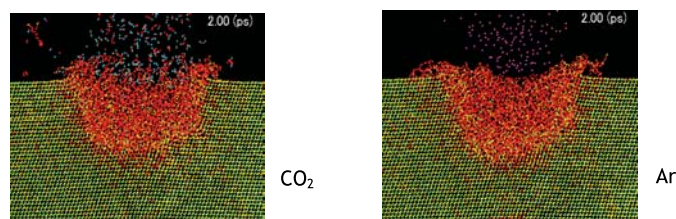


**Fig. 5.** Relaxed impact craters of CO<sub>2</sub> or Ar clusters in diamond at 2.00 ps after the impact, according to molecular dynamics simulations, showing the more compact relaxation after the Ar cluster impact.

#### 4 Molecular dynamics simulations of single cluster impacts

In order to compare with the nanofriction results of the cluster erosion, some molecular dynamics simulation results of single cluster impacts on diamond (111) are presented. Detailed reports of these simulations have been reported elsewhere [5, 7].

The impacts of Ar clusters with 961 atoms, or of CO<sub>2</sub> clusters with 960 molecules, respectively, with an initial kinetic cluster energy of 100 keV onto a (111) surface of a hexagonal single crystal diamond specimen of 18.2 nm thickness and 34.4 nm diagonal width have been simulated.

Figure 5 shows a comparison of the relaxation of the craters formed directly after the impact of a CO<sub>2</sub> cluster, or of an Ar cluster, respectively. A slice of the sample of only 1 nm thickness in the direction perpendicular to the figure plane and containing the impact trajectory is presented in order to clarify the crater cross section. Shortly after the impact the transient craters are nearly indistinguishable. At 2 ps after the impact, however, to which time Figure 5 refers, the crater formed by an Ar cluster impact is filled up in a rather smooth and compact way, while the CO<sub>2</sub> interaction leads to a more loose packing with a rather disrupted surface. Although it is not possible to infer from these short-time simulations the surface friction

properties to be expected finally for much longer times, the tendency toward a rougher, less compact surface after a high-speed impact of a CO<sub>2</sub> cluster, as compared to an Ar cluster impact, seems to be illustrated.

#### 5 Discussion

The sequential erosion of synthetic single crystal diamond by first CO<sub>2</sub>, then Ar clusters has been found to yield the lowest friction surface in contact with a silicon nitride cantilever. Ar cluster erosion alone yields practically the same value, however. CO<sub>2</sub> cluster erosion alone yields about 8 times higher friction than Ar cluster erosion. The sequential erosion allows to combine favorably the four times higher erosion rate of RACE, the CO<sub>2</sub> cluster erosion [5], with the low friction surface finish of the Ar cluster erosion. These results are in accordance with the previous roughness measurements of the respective surfaces [5] although the ratio of the friction values is even higher than the ratio of about 4 reported for the roughness values.

This work was supported by the Forschungszentrum Karlsruhe, Technik und Umwelt, Germany, and by a Grant-in-Aid for JSPS Fellows (No. 11-08826) from the Ministry of Education, Science, Sports and Culture, Japan.

#### References

1. K. Shinjo, M. Hirano, *Surf. Sci.* **283**, 473 (1993)
2. M. Dienwiebel et al., *Phys. Rev. Lett.* **92**, 126101 (2004)
3. P.R.W. Henkes, R. Klingelhöfer, *J. Phys. (Paris)* **50**, C2-159 (1989)
4. J. Gspann, *Microelectr. Engineer.* **27**, 517 (1995)
5. R. Krämer, Y. Yamaguchi, J. Gspann, *Surf. Interf. Anal.* **36**, 148 (2004)
6. J. Ruan, B. Bushan, *ASME J. Tribol.* **116**, 378 (1994)
7. C. Becker, J. Gspann, R. Krämer, Y. Yamaguchi, *Chin. Phys.* **10**, S174 (2001)